Underdetermined Blind Source Separation of Bioacoustic Signals

Norsalina Hassan[1] and Dzati Athiar Ramli[2]*

[1]Department of Electrical Engineering, Politeknik Seberang Perai, 13700 Jalan Permatang Pauh, Pulau Pinang, Malaysia
[2]School of Electrical & Electronic Engineering, Universiti Sains Malaysia, Nibong Tebal, 14300, Pulau Pinang, Malaysia

ABSTRACT

Bioacoustic signals have been used as a modality in environmental monitoring and biodiversity research. These signals also carry species or individual information, thus allowing the recognition of species and individuals based on vocals. Nevertheless, vocal communication in a crowded social environment is a challenging problem for automated bioacoustic recogniser systems due to interference problems in concurrent signals from multiple individuals. The bioacoustics sources are separated from the mixtures of multiple individual signals using a technique known as Blind source separation (BSS) to address the abovementioned issue. In this work, we explored the BSS of an underdetermined mixture based on a two-stage sparse component analysis (SCA) approach that consisted of (1) mixing matrix estimation and (2) source estimation. The key point of our procedure was to investigate the algorithm's robustness to noise and the effect of increasing the number of sources. Using the two-stage SCA technique, the performances of the estimated mixing matrix and the estimated source were evaluated and discussed at various signal-to-noise ratios (SNRs). The use of different sources is also validated. Given its robustness, the SCA algorithm presented a stable and reliable performance in a noisy environment with small error changes when the noise level was increased.

Keywords: Bioacoustic signals, blind source separation, sparse component analysis, underdetermined mixtures

INTRODUCTION

Bioacoustics can be defined as the study of animal sound communication and can be considered one of the most effective methods in environmental monitoring applications and biodiversity research (Huang et al., 2009). In particular, vocalising

animals, such as frogs, primarily rely on sound to interact with conspecies or other species by making a range of different calls for various purposes. Humans can use such sounds to extract additional detailed species information and identify species (Stevenson et al., 2015). Most studies on animal call recognition focused on animal species identification. However, identifying different animal species in accordance with recorded calls, which frequently contain vocalisations from more than one individual, is difficult (Hassan & Ramli, 2018). This situation makes identifying the source data from a given mixture of data challenging. Therefore, postprocessing approaches are needed to separate individual bioacoustic sources from sound mixtures to enhance the process further. Blind source separation (BSS) is often used in audio, digital communication, biomedical, and signal processing to separate source signals from mixed signals (Santamaria, 2013).

Depending on the number of sources, N and the number of sensors, M, BSS can be classified into determined ($N = M$), overdetermined ($N < M$) and underdetermined ($N > M$) cases. In determined cases, the mixing matrix A can be invertible as it is a square matrix. Therefore, the source can be recovered easily by multiplying the mixture with the inverse of A after discovering the mixing matrix. Independent component analysis is a well-known method for determining cases (Hyvarinen, 2012). For overdetermined cases, the mixing matrix can be transformed into a square using principal component analysis (Winter et al., 2006). Underdetermined cases are the most popular among these three cases because they best fit the practical application. For underdetermined mixtures cases, the mixing matrix is not square and is therefore insufficient for reconstructing the sources because of the noninvertible mixing matrix. Therefore, the algorithms used for the determined and overdetermined cases may not work when dealing with a complex problem, such as underdetermined mixtures. Therefore, important prior information from sources, such as sparsity, is required to resolve the underdetermined problem. If an appropriate linear transformation is applied, the sources not sparse in the time domain can be sparse in the time-frequency (TF) domain. Some algorithms for achieving sparsity in the transform domain, namely short-time Fourier transform (STFT) (Linh-Trung et al., 2005; Lu et al., 2019; Su et al., 2017) and wavelet packet transform (Li et al., 2003; Miao et al., 2021; Sadhu et al., 2011), have been proposed thus far.

The main method for underdetermined cases is Sparse Component Analysis (SCA) (Li et al., 2003). Most existing SCA algorithms that exploit the sparse representation of the mixtures $X(t)$ are composed of two stages, as shown in Figure 1.

The underdetermined problem is solved by estimating the sources from the observed signals using the mixing matrix estimated in the first stage. If the mixing matrix is identified as inaccurate, the source cannot recover. Hence, the first stage is very important. The mixing matrix estimation method can further be classified into two categories, i.e., single source point (SSP) detection and clustering. In the second stage, a series of least-squares
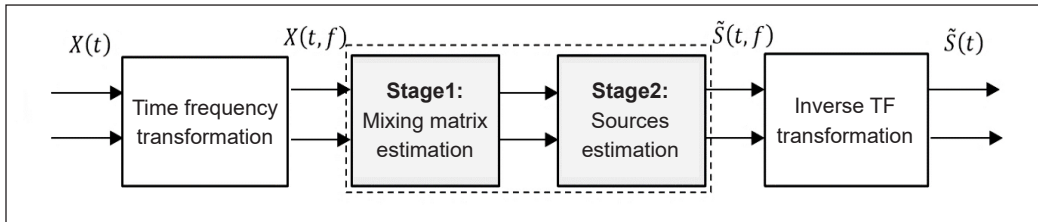
Figure 1. Two-stage method for SCA

problems is used to recover the estimated sources. Recently, many studies have focused on underdetermined problems based on the SCA framework. For example, the works of (Reju et al., 2009) identified SSPs by the fact that the absolute orientations of the real and imaginary sections of the Fourier transform coefficient vectors of the mixed signals are the same. The detected SSPs are then used to estimate the mixing matrix using hierarchical clustering. Finally, the degenerate unmixing estimation algorithm introduced by (Jourjine et al., 2000) recovers the source signals based on the ratio of the observed mixing signals' TF transforms.

The performances of the algorithms (Jourjine et al., 2000; Reju et al., 2009) depend on this ratio to detect SSPs. (Li et al., 2016) present an improved algorithm by utilising the TF coefficients of the mixed signals and complex conjugates of the coefficient for identifying SSPs. On the other hand, most SSPs-based underdetermined mixtures only consider a single SSP and ignore the relationship between SSPs. As a result of this situation, SSPs have low identification accuracy, particularly in noisy cases. The work of (Zhen et al., 2017) introduced blind source separation for underdetermined mixtures based on STFT, with SSPs identified using sparse coding. This method can exhibit excellent estimation performance even in low signal-to-noise ratio (SNR) cases, as the sparse coding strategy considers the linear relations between SSPs. This work aims to investigate the performance of BSS for underdetermined mixtures using the method of (Zhen et al., 2017) on our bioacoustic signals. As in real life, the underdetermined mixtures are formed by a pair of random mixing matrices with different selected source vectors. The mixture of sources is dynamic because the position of sources and the sensors are subject to change with time.

METHODOLOGY

The underdetermined mixtures' linear instantaneous mixed model can be written as Equation 1:

$$X(t) = AS(t), \qquad\qquad [1]$$

where $X(t) = [X_1, X_2, ..., X_M]^T$ and $S(t) = [S_1, S_2, ..., S_N]^T$ are the vectors of the mixtures and sources in the time domain of transposition operation. M and N are the numbers of

mixed and source signals, respectively, where M is lesser than N. $A = [a_1, a_2, ..., a_N]$ is the mixing matrix. The entries of each matrix A are determined by several characteristics, which include source locations, sensor locations, and acoustical properties. The BSS of underdetermined mixtures aims to estimate the source signals when A and S are unknown.

Data Preparation

Seven bioacoustic sources from an in-house database are used in this experiment. Figure 2 presents the dataset of the bioacoustic signals $S_N(t)$ employed in this study. The species name of each source is given below:

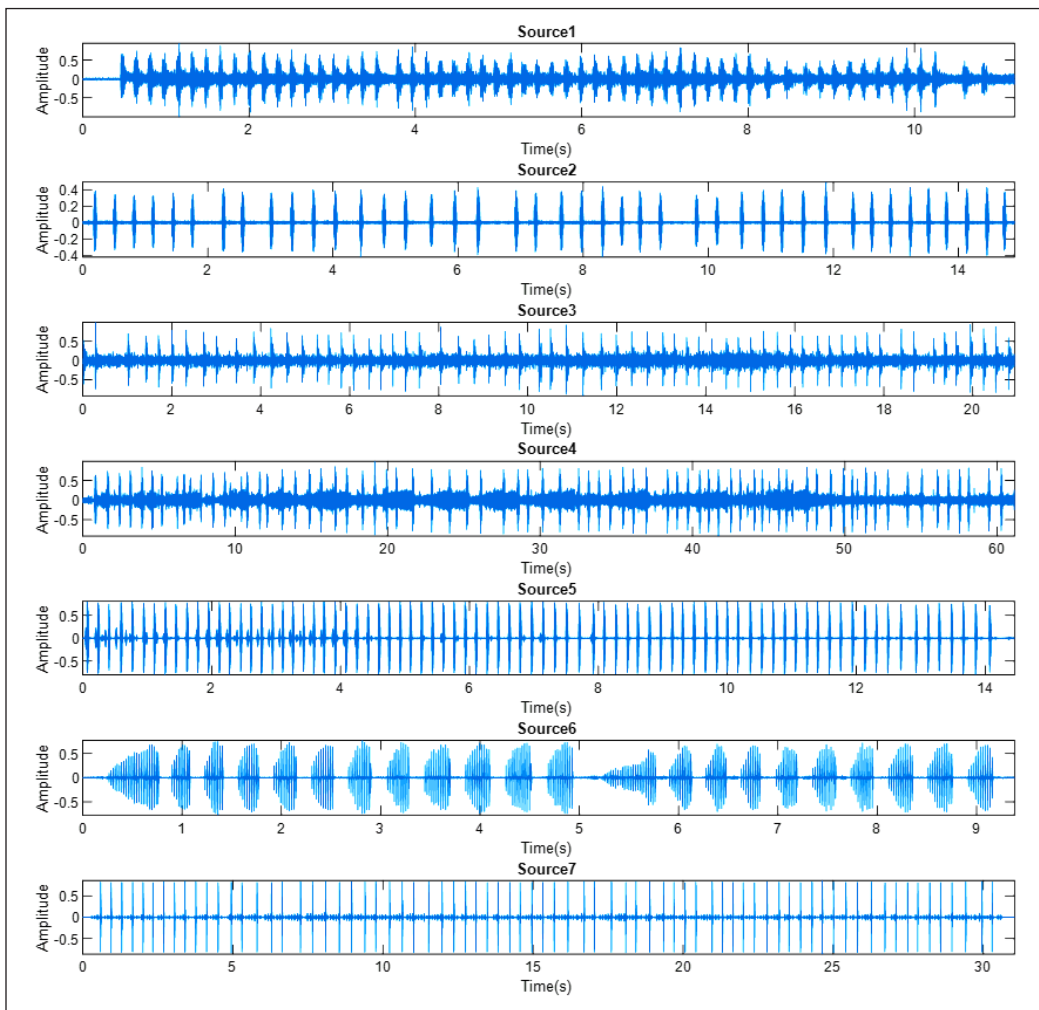Source 1: *Ameerega trivittata*
Source 2: *Adenomera andre*

Figure 2. Dataset of bioacoustic source signals

Source 3: *Leptodactylus hylaedactylus*

Source 4: *Leptodactylus fuscus*

Source 5: *Geocrinia victoriana*

Source 6: *Geocrinia victoriana*

Source 7: *Limnodynastes convexiusculus*

The signals were recorded in wav format in the monochannel at 16-bit and 16 kHz.

Mixed Signal Generation

In a real-life environment, the nature of mixtures varies in accordance with the position of animals and sensors. Mixed signals were generated using Equation 1 with the random selection of sources from 1: N and with a random mixing matrix ($M \times N$) to mimic the behaviour of the real-life system. Each nerated mixed signal $X(t)$ had a different entry of sources and mixing matrix. To our knowledge, no standard way exists for the dynamic/nonstatic underdetermined mixtures of bioacoustic signals. In our case, the term dynamic indicates that the sources and weight are not static but subject to change. Therefore, we decided to create one based on our data through the procedure illustrated in Figure 3. Here, A represents the weight from a source to a sensor, and the different selections of sources represent the different locations of sources.
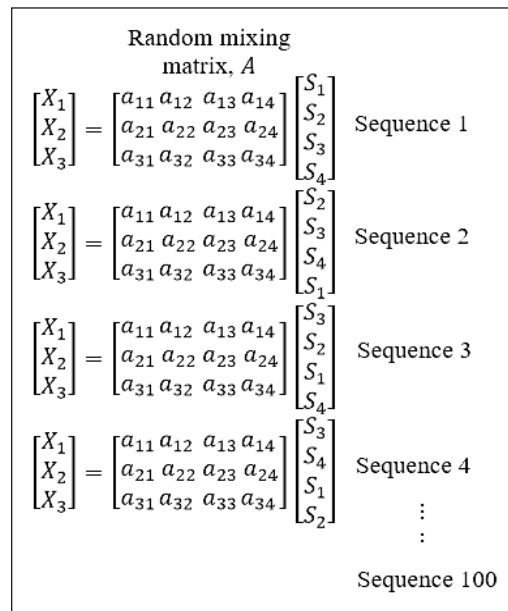

Figure 3. The procedure of mixed-signal generation

Domain Transformation

Natural signals, such as bioacoustic ones, are sparse in the time domain. Therefore, the STFT transformation was applied to Equation 1 to increase the sparsity of source signals. The STFT of the m-th mixture $x_m(t)$ is given by Equation 2:

$$X_m(t,f) = \int_{-\infty}^{\infty} x_m(\tau)h(t-\tau)e^{-j2\pi f\tau}\,d\tau \qquad [2]$$

where $h(t)$ is the window function. Given that A is constant and that STFT is used on both sides of Equation 1, the mixing model in the time-frequency domain is obtained as Equation 3:

$$\tilde{X}(t,f) = A\tilde{S}(t,f) \qquad\qquad [3]$$

w h e r e $\tilde{X}(t,f) = [\tilde{X}_1(t,f), \tilde{X}_2(t,f), \ldots, \tilde{X}_M]^T$ a n d $\tilde{S}(t,f) = [\tilde{S}_1(t,f), \tilde{S}_2(t,f), \ldots, \tilde{S}_N]^T$ represent the STFT complex coefficients of $X(t)$ and $S(t)$ at TF point (t,f), respectively. The underdetermined mixtures in the time domain and the TF domain of three mixtures and four sources are illustrated in Figures 4 and 5, respectively. Figure 4 shows that the mixtures' direction is unclear due to the sources' weak sparsity. After the STFT is addressed, the scatter plot in Figure 5 clearly shows the column directions of the mixing matrix.
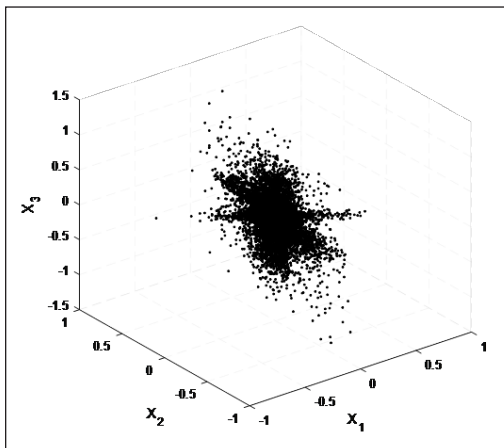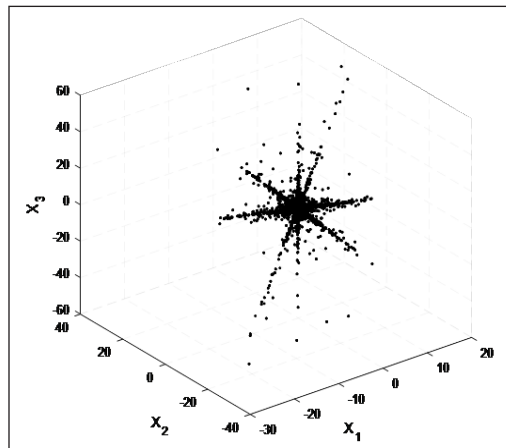

Figure 4. Mixed bioacoustic signals in the time-domain   *Figure 5*. Mixed bioacoustic signals in the TF domain

The Mixing Matrix Estimation

The mixing matrix was estimated using the TF domain mixing model. Mixing matrix estimation is an important procedure in SCA and can be improved in two ways: SSP detection and clustering. Two assumptions were made to estimate the mixing matrix:

A1) Any column vector is linearly independent in the mixing matrix A.

A2) There are some TF points (t,f) for each source s_i' in which only s_i' is dominant, $|\tilde{S}_i(t,f)| \geq |\tilde{S}_j(t,f)| \forall_j \neq i$.

The stability of SSP detection can be increased by using both assumptions. The steps of mixing matrix estimation can be summarised as follows:

1. Generate the underdetermined mixtures.
2. Transform the time domain underdetermined mixtures $X(t)$ into the TF domain $\tilde{X}(t,f)$.
3. Detect the SSP: Compute the sparse coding coefficients
4. Through l_1-norm optimisation to detect the SSP for each of the TF vectorisation. The problem of sparse coding can be formulated as Equation 4:

$$J(c_i : \lambda) = \frac{1}{2} \|y_i - Y_{C_i}\|_2^2 + \lambda \|c_i\|_1 \ s.t c_{ii} = 0, \qquad [4]$$

where c_i is the $\|c_i\|_1$ l_1-norm and $y_i - Y_{C_i}$ is the reconstruction error between each mixture TF vector and the linear combination of it. The SSP is the sparse coding coefficient with only one nonzero element at the TF point.

Apply the hierarchical clustering technique to the detected single-source mixture TF vectors to obtain clustering centres, which can then be used to calculate the estimated mixing matrix $\tilde{A}$.

The Source Recovery Estimation

Following the estimation of the mixing matrix, the bioacoustic source $\tilde{S}$ is estimated. Given that Equation 1 is underdetermined, its solution is not unique even when $\tilde{A}$ is known. Assumption A2 is needed to achieve source recovery. Let A be a set consisting of all $Mx(M-1)$ submatrices of $\tilde{A}$ (Equation 5):

$$\boldsymbol{A} = \{\boldsymbol{A_i} | \boldsymbol{A_i} = [\ \widehat{\boldsymbol{a}}_{\boldsymbol{\theta_1}}, \widehat{\boldsymbol{a}}_{\boldsymbol{\theta_2}, \dots}, \widehat{\boldsymbol{a}}_{\boldsymbol{\theta_{M-1}}}\ ]\}. \qquad [5]$$

Then, for any TF point (t, f) there must exist a matrix element $\boldsymbol{A_*} = \{\boldsymbol{A_i} | \boldsymbol{A_i} = [\ \widehat{\boldsymbol{a}}_{\boldsymbol{\theta_1}}, \widehat{\boldsymbol{a}}_{\boldsymbol{\theta_2}, \dots}, \widehat{\boldsymbol{a}}_{\boldsymbol{\theta_{M-1}}}\ ]\}$ that fulfils Equation 6:

$$\widetilde{X}(t, f) = \boldsymbol{A_*} \boldsymbol{A_*}^{\dagger} \widetilde{X}(t, f), \qquad [6]$$

where $\dagger$ is the pseudoinverse of $\boldsymbol{A_*}$. Then, Equation 7 can estimate source signals:

$$\tilde{S}_j(t, f) = \begin{cases} i, & if \ j = \emptyset_1 \\ 0, & otherwise \end{cases}, \qquad [7]$$

where $e = [e_1, e_2, \dots, e_{M-1}]^T = \boldsymbol{A_*}^{\dagger} \widetilde{X}(t, f)$ and $\boldsymbol{A_*}$ is produced by Equation 8:

$$\boldsymbol{A_*} = \underset{\boldsymbol{A_i} \in A}{arg\ min} \|\widetilde{X}(t, f) - \boldsymbol{A_*} \boldsymbol{A_*}^{\dagger} \widetilde{X}(t, f)\|_2. \qquad [8]$$

Finally, using inverse STFT, the time domain of the estimated bioacoustic signal S (t) can be easily obtained.

RESULTS AND DISCUSSION

Experimental Setup

For the experimental setup, randomly selected sources from 1: N of $S(t)$ were mixed with 100 random mixing matrices using Equation 1 to generate 100 random mixtures $X(t)$.

This setup was intended to represent a real environment wherein some sensors are placed in different positions to receive mixed signals. The algorithm was implemented on each mixture signal to separate the bioacoustic source signals. The STFT size of each mixture signal was set to 1024 with the time step was 512, and the weighting function was a Hamming window. The averages of 100 Monte Carlo simulation tests were obtained to evaluate the performance of the SCA method. We performed the following at each stage of the SCA algorithm:

    (1) We investigated the algorithm's robustness concerning the noise by evaluating system performance at different SNRs. Compared to background noise, SNR is a metric that measures the level of the desired signal with that of the background.

    (2) We also assessed the algorithm's performance by using the setting of different numbers of mixtures M and the numbers of sources N where $M{\times}N = 3{\times}4$, $3{\times}5$, $3{\times}6$, $4{\times}5$, $4{\times}6$.

$3{\times}4$, $3{\times}5$ and $3{\times}6$ indicate that four, five, and six sources are received by three sensors, respectively, whereas $4{\times}5$, $4{\times}6$, and $4{\times}7$ indicate that five, six and seven sources are received by four sensors, respectively.

First Stage: Performance of Mixing Matrix Estimation

The following Equation 9 was used to quantify the performance of mixing matrix estimation:

$$Error \ = \ \frac{1}{N}\sum_{t-1}^{n}(1 \ - \ \frac{a_i^T \widehat{a}_i}{\|a_i\|\|\widehat{a}_i\|}),$$ [9]

where the number of sources is represented by N and $\widehat{a}_i$ represents the estimation of mixing vector $\widehat{a}_i$. As the error decreases, the accuracy of mixing matrix estimation increases. Gaussian white noise is added to the mixed signal to compare how robust the method is to noise. The noise performance of the algorithm at various signal-to-noise ratios (SNR) ranging from 5 dB to 45 dB was tested.

    Figures 6 and 7 show the averaged error obtained by 100 Monte Carlo tests in estimating the mixing matrix for three and four mixtures with different numbers of sources, respectively. As inferred from Figure 6, the error values tended to decrease as the SNR was increased in all settings. Figure 7 also illustrates the same trend. This result indicated that the mixing matrix's accuracy improved as the SNR value was increased. The robustness of SCA concerning noise was demonstrated here, given that it presented a stable and reliable performance when the noise level was increased from 45 dB to 5 dB with error changes less than 0.15. Comparing the performances of different settings in Figures 6 and 7 revealed that the three mixture settings obtained small average errors at the SNR of 45 dB. This result showed that mixing matrix estimation in the three-mixture setting was superior to that in the four-mixture setting. Figures 6 and 7 illustrated that the performances under

different sensor settings degraded when the number of sources was increased. This finding indicated that the number of sources and sensors strongly correlates with performance.

Next, the three-mixture setting using Zhen's method, which utilised sparse coding to identify the SSPs, was chosen for a quantitative comparison in estimating the mixing matrix with V.G. Reju's (Reju et al., 2009) and the TIFROM (Abrard & Deville, 2005) methods. We applied the same setting to both comparison methods. Figure 8 compares the performance of different mixing matrix estimation methods after 100 Monte Carlo trials for bioacoustic signals. Observing the error with changes in SNR from 5 to 45dB shows that all errors from different approaches diminish with rising SNR for bioacoustic

signals. The estimation performance of V.G. Reju, TIFROM and the method proposed by Zhen differs significantly when the SNR is less than 30 dB. All methods have lower estimation performance when the SNR is greater than 30dB. The three-mixture setting using Zhen's method has a more consistent and dependable performance. In the noisy case, the three-mixture setting using Zhen's method outperforms V.G. Reju and TIFROM by more than 0.5dB in error when SNR declines from 45dB to 5dB. The suggested technique provides a low error rate when implemented for bioacoustic signals.
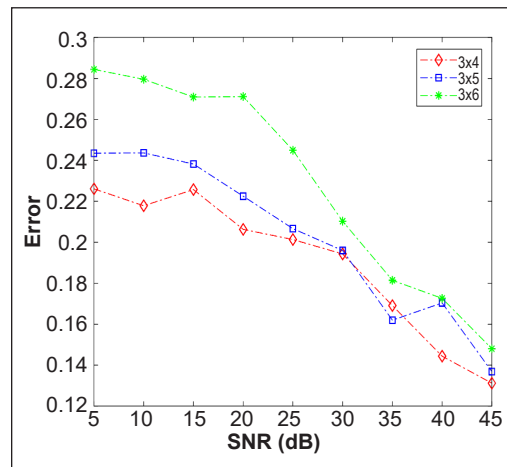

Figure 6. Comparison of the mixing matrix estimation performances of three mixtures with different numbers of sources at different SNRs
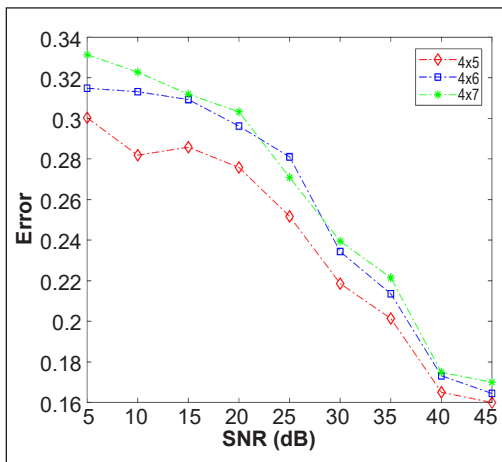

Figure 7. Comparison of the mixing matrix estimation performances of four mixtures with different numbers of sources at different SNRs
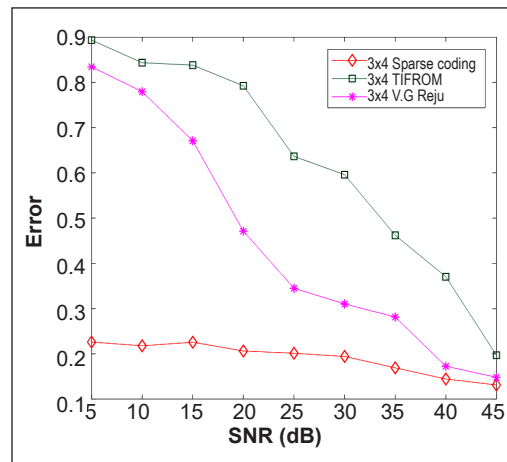

Figure 8. Comparison of the mixing matrix estimation performances of three mixtures for different methods at different SNRs

Second Stage: The Source Recovery Estimation

After estimating the mixing matrix, the source recovery was quantified. The accuracy of source recovery is determined by how well we estimate the mixing matrix. The quality of the separation was tested by using the following measures to achieve bioacoustic source recovery (Equation 10):

$$Mean\ Squared\ Error, MSE\ = 10log_{10}(\frac{1}{n}\sum_{t=1}^{nt} \min_{\delta} \frac{\|s_i' - \delta \tilde{s}_i'\|_2^2}{\|s_i'\|_2^2}), \qquad [10]$$

where s_i' represents the *ith* source, $\tilde{s}_i'$ is the estimated source, and δ is a scalar that reflects the scalar ambiguity. Figures 9 and 10 show the comparison of the performances of the three and four mixtures with different numbers of sources in source recoveries at different SNRs. The average results were taken from 100 Monte Carlo simulations. The trend in Figures 9 and 10 showed that as the SNR was increased, the MSE decreased under all settings, in agreement with the finding reported by (Zhen et al., 2017). At 45dB SNR, the three-mixture setting provided a smaller MSE value than the four-mixture setting. A small MSE indicates high accuracy in source recovery. Figures 9 and 10 indicate that accuracy degraded when the number of sources was increased. When additional sources were used, the performance degradation may be attributed to the difficulty in satisfying the restriction in assumption A2, wherein only one source is active at any TF point.

We evaluated performance by using three metrics, namely, signal-to-distortion ratio (SDR), signal-to-interferences ratio (SIR), and signal-to-artefacts ratio (SAR), to measure the quality of the separated bioacoustic source signals (Vincent et al., 2006). High values of the metrics indicate good quality of separation. The results summarised in Figure 11
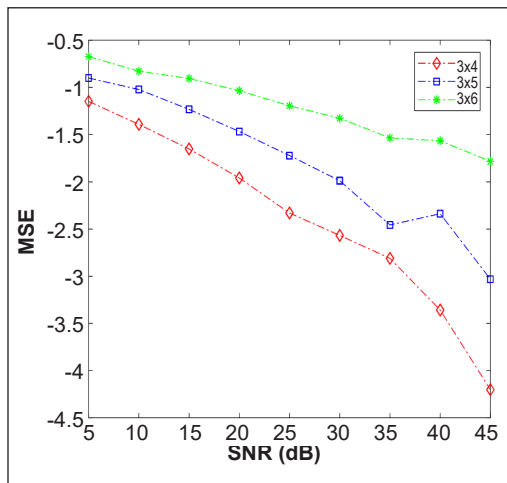
Figure 9. Comparison of source recovery performances by the three-mixture setting with different numbers of sources at different SNRs
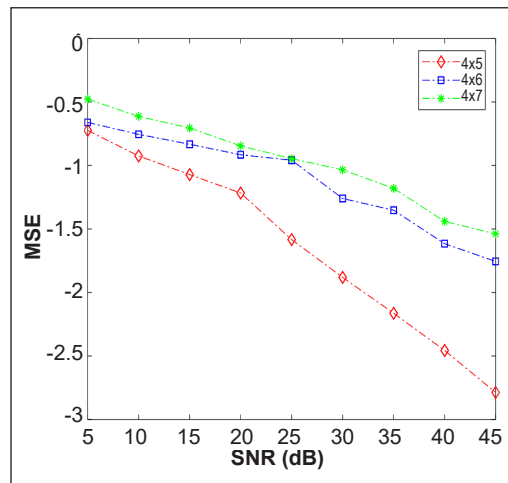
Figure 10. Comparison of the source recovery performances of the four-mixture setting with different numbers of sources at different SNRs

demonstrated that 3×4 and 3×5 exhibited high SDR, SIR, and SAR values under all settings, thus showing that the sources were well separated. On the other hand, the 3×6 setting obtained low SDR and SIR values for Source 2. This situation showed that the increasing number of sources does impact the source recovery performance. Figure 12 depicts that for each setting, 4×5 can separate all the sources well, whereas the setting for 4×6 can only separate sources 2 and 3, and 4×7 can only separate source 1. In short, the discrepancy between the number of sources and the number of sensors influences the separation performance of our underdetermined bioacoustic mixtures.

Some simulation results are also presented to illustrate the performance of the separation algorithms. The simulation results related to the performance in Figure 11 are shown in Figures 13, 14, and 15. Figure 13 presents the simulation result of separating four sources from three mixtures. All estimated sources were sufficiently close to the sources. Figure 14 provides the simulation result of separating five sources from three mixtures. Given the simulation results, the estimated source 5 was not fully recovered but can still be identified as source 5. Figure 15 gives the simulation result of separating six sources from three mixtures, indicating that four sources were effectively recovered while source 2 was incompletely recovered. The simulation results related to the performance depicted in Figure 12 are shown in Figures 16, 17, and 18, illustrating the results of separating five, six, and seven sources from four mixtures, respectively. In Figure 16, all estimated sources were fully recovered except for estimated source 5. Figure 17 shows that only estimated sources 2 and 4 were recognisable. Meanwhile, in Figure 18, only estimated source 1 was recovered. The results indicated that the SCA algorithm using our bioacoustic signals performed best with three mixtures with increasing numbers of sources at different SNRs.
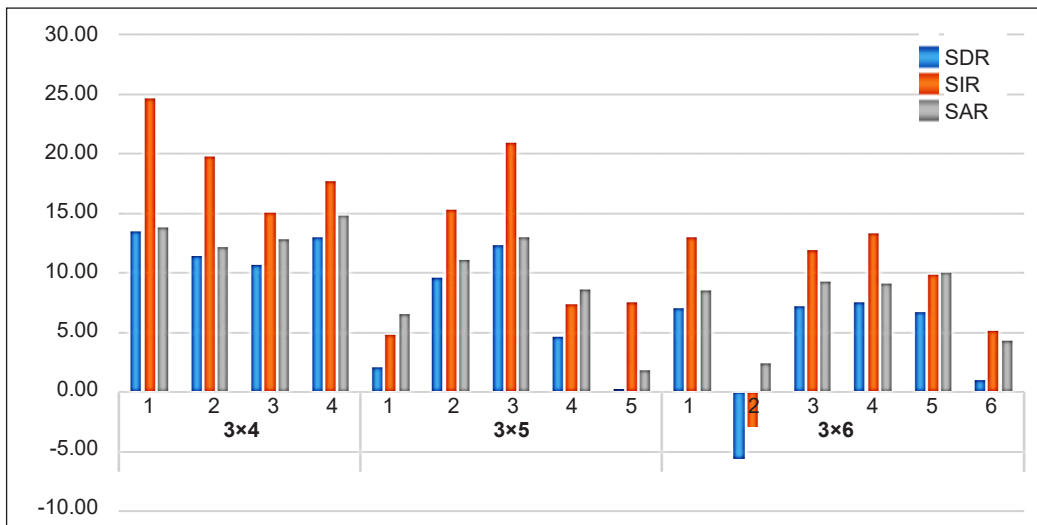

Figure 11. Comparison of the bioacoustic signal separation performances of three mixtures with different numbers of sources
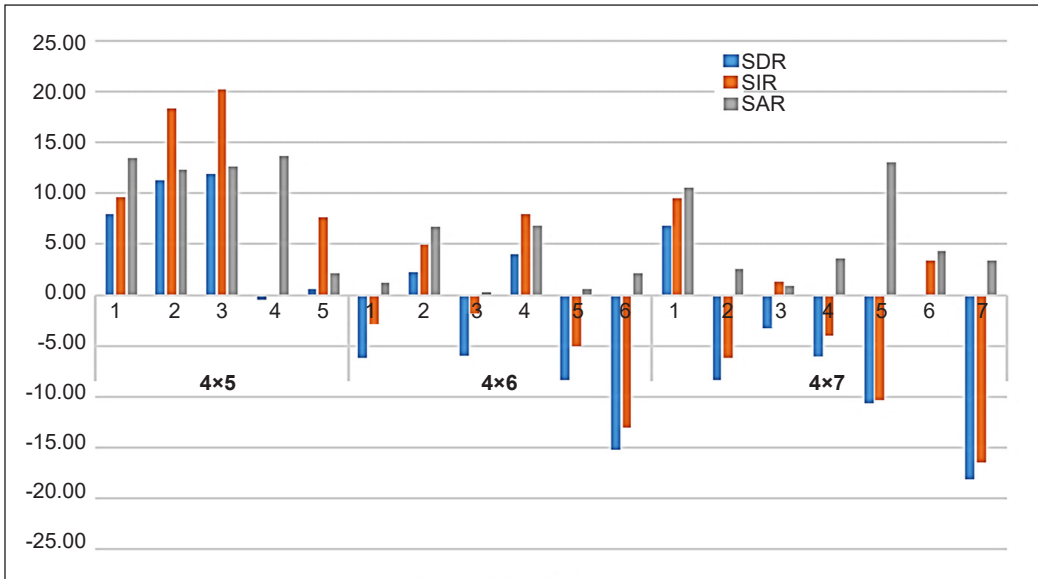
Figure 12. Comparison of the bioacoustic signal separation performances of four mixtures with different numbers of sources
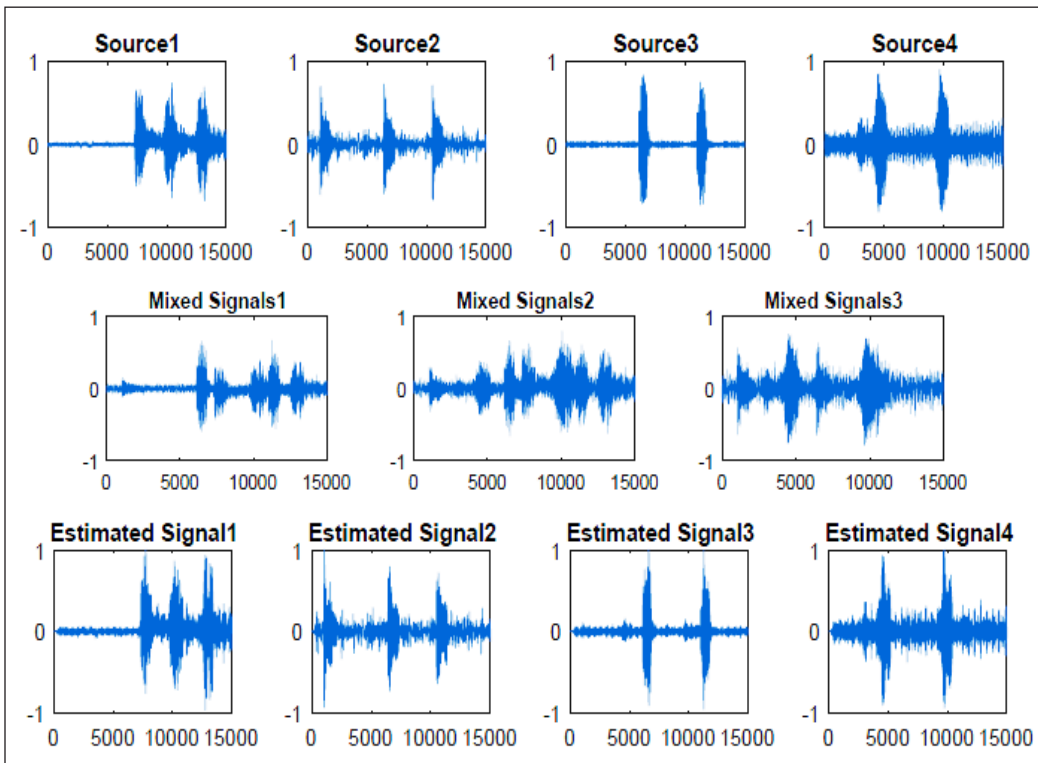

Figure 13. Simulation result of the separation of four sources from three mixtures. First row: Bioacoustic source signals. Second row: Mixtures. Third row: Estimated source signals
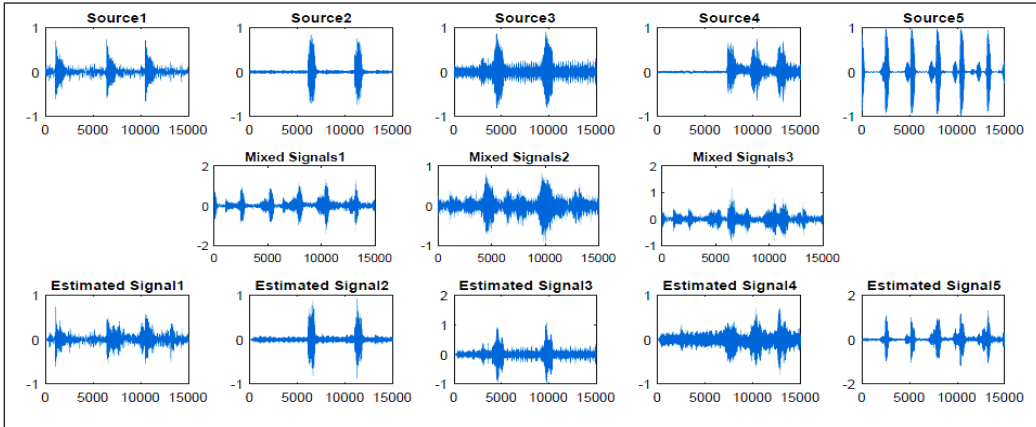
Figure 14. Simulation result of separating five sources from three mixtures. First row: Bioacoustic source signals. Second row: Mixtures. Third row: Estimated source signals
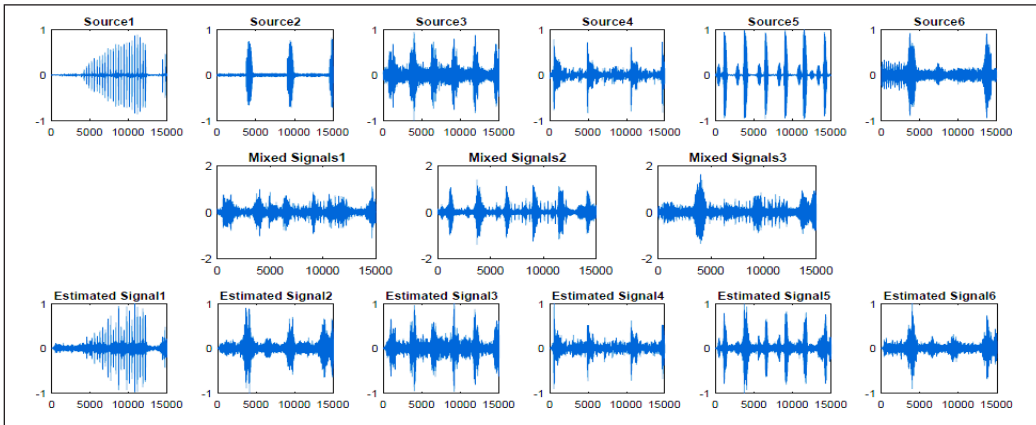

Figure 15. Simulation result of separating six sources from three mixtures. First row: Bioacoustic source signals. Second row: Mixtures. Third row: Estimated source signals
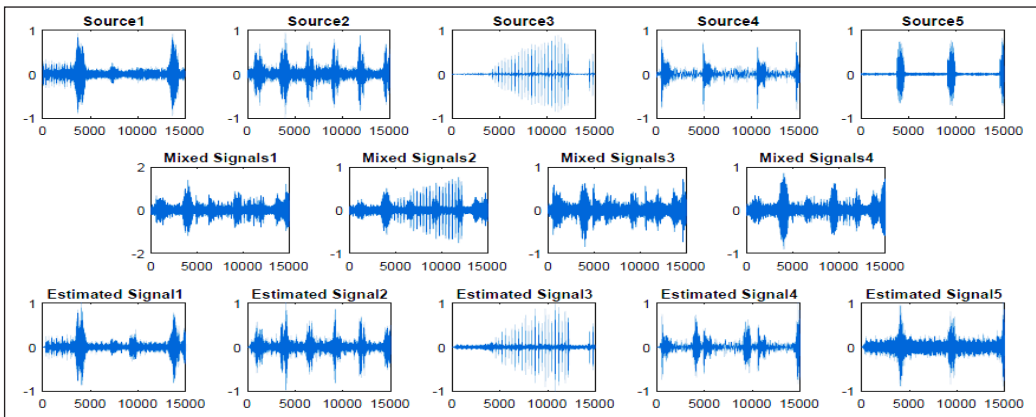

Figure 16. Simulation result of separating five sources from four mixtures. First row: Bioacoustic source signals. Second row: Mixtures. Third row: Estimated source signals

Figure 17. Simulation result of separating six sources from four mixtures. First row: Bioacoustic source signals. Second row: Mixtures. Third row: Estimated source signals
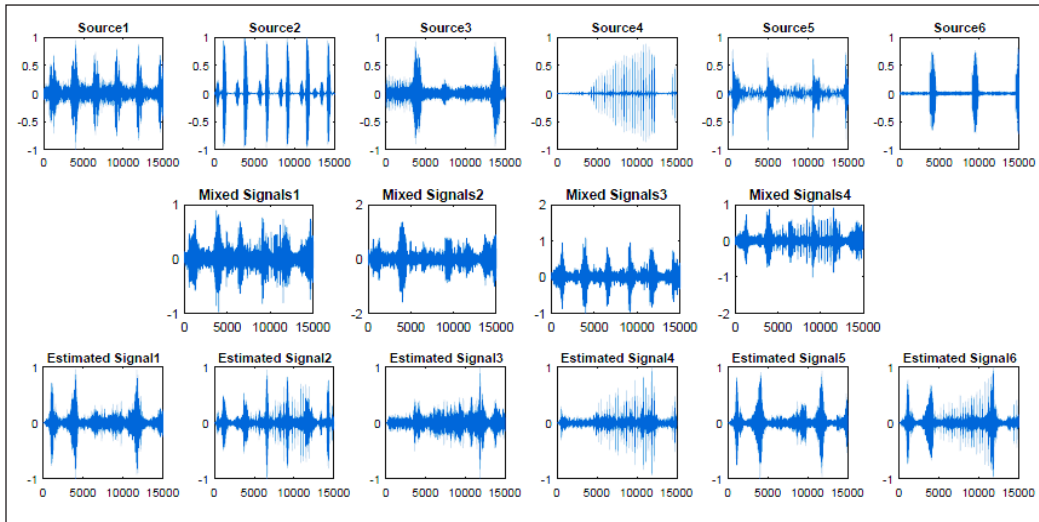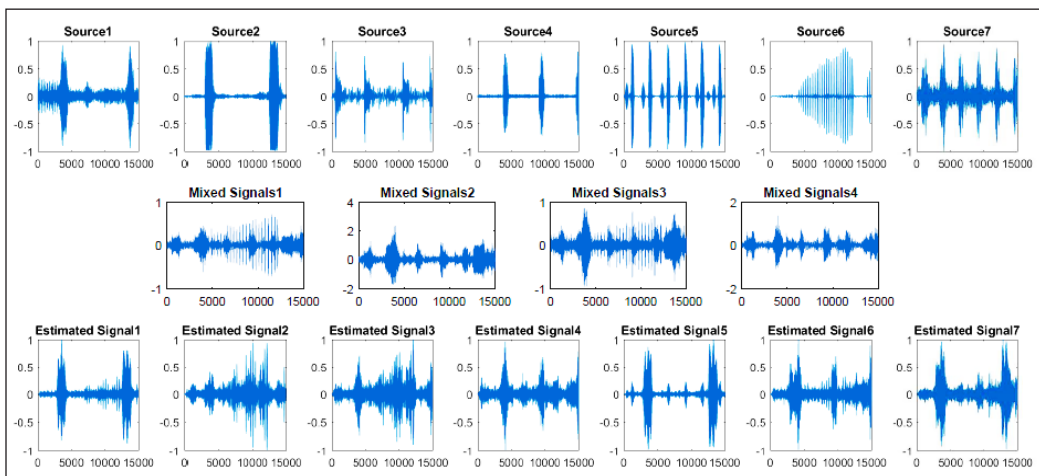

Figure 18. Simulation result of separating seven sources from four mixtures. First row: Bioacoustic source signals. Second row: Mixtures. Third row: Estimated source signals

CONCLUSION

This study exploited the SCA algorithm miming the real environment procedure for underdetermined bioacoustic mixtures. The sources in the underdetermined mixtures presented here exhibited sparse behaviour after being transformed into the TF domain using STFT. SSPs were discovered by estimating the mixing matrix with sparse coding. A series of least-square problems were used to recover the estimated sources. The robustness of the SCA algorithm also demonstrated that the algorithm presented a stable and reliable

performance in a noisy environment with small error changes when the SNR was increased. The influences of different numbers of sources and sensors on the SCA algorithm were examined. The experimental results revealed that the performances varied when different numbers of sources and sensors were used. Moreover, the performances of the SCA algorithm using bioacoustic signals degraded when the number of sources was increased, and the number of sensors was fixed.

ACKNOWLEDGEMENT

REFERENCES

Abrard, F., & Deville, Y. (2005). A time–frequency blind signal separation method applicable to underdetermined mixtures of dependent sources. *Signal Processing*, *85*(7), 1389-1403. https://doi.org/10.1016/j.sigpro.2005.02.010

Hassan, N., & Ramli, D. A. (2018). A Comparative study of blind source separation for bioacoustics sounds based on FastICA, PCA and NMF. *Procedia Computer Science*, *126*, 363-372. https://doi.org/10.1016/j.procS.2018.07.270

Huang, C. J., Yang, Y. J., Yang, D. X., & Chen, Y. J. (2009). Frog classification using machine learning techniques. *Expert Systems with Applications*, *36*(2), 3737-3743. https://doi.org/10.1016/j.eswa.2008.02.059

Hyvarinen, A. (2012). Independent component analysis: Recent advances. *Philosophical Transactions of the Royal Society A: Mathematical, Physical and Engineering Sciences*, *371*(1984), 20110534-20110534. https://doi.org/10.1098/rsta.2011.0534

Jourjine, A., Rickard, S., & Yilmaz, O. (2000, June 5-9). *Blind separation of disjoint orthogonal signals Demixing n sources from 2 mixtures*. [Paper presentation]. 2000 IEEE International Conference on Acoustics, Speech, and Signal Processing. Proceedings (Cat. No. 00CH37100), Istanbul, Turkey. https://doi.org/10.1109/ICASSP.2000.861162

Li, Y., Cichocki, A., & Amari, S. I. (2003, April 1-4). *Sparse component analysis for blind source separation with less sensors than sources*. [Paper presentation]. 4th Internation Symposium on Independent Component Analysis and Blind Signal Separation (ECA2003), Nara, Japan.

Li, Y., Nie, W., Ye, F., & Lin, Y. (2016). A mixing matrix estimation algorithm for underdetermined blind source separation. *Circuits, Systems, and Signal Processing*, *35*(9), 3367-3379. https://doi.org/10.1007/s00034-015-0198-y

Linh-Trung, N., El Bey, A. A., Abed-Meraim, K., & Belouchrani, A. (2005, August 28-31). *Underdetermined blind source separation of non-disjoint nonstationary sources in the time-frequency domain*. [Paper presentation]. 8th International Symposium on Signal Processing and its Applications, (ISSPA), Sydney, Australia. https://doi.org/10.1109/ISSPA.2005.1580192

Lu, J., Cheng, W., He, D., & Zi, Y. (2019). A novel underdetermined blind source separation method with noise and unknown source number. *Journal of Sound and Vibration*, *457*, 67-91. https://doi.org/10.1016/j.jsv.2019.05.037

Miao, F., Zhao, R., Jia, L., & Wang, X. (2021). Multisource fault signal separation of rotating machinery based on wavelet packet and fast independent component analysis. *International Journal of Rotating Machinery*, *2021*, Article 9914724. https://doi.org/10.1155/2021/9914724

Reju, V. G., Koh, S. N., & Soon, I. Y. (2009). An algorithm for mixing matrix estimation in instantaneous blind source separation. *Signal Processing*, *89*(9), 1762-1773. https://doi.org/10.1016/j.sigpro.2009.03.017

Sadhu, A., Hazra, B., Narasimhan, S., & Pandey, M. D. (2011). Decentralized modal identification using sparse blind source separation. *Smart Materials and Structures*, *20*(12), Article 125009. https://doi.org/10.1088/0964-1726/20/12/125009

Santamaria, I. (2013). Handbook of blind source separation: Independent component analysis and applications (Common, P. and Jutten, ; 2010 [Book Review]. *IEEE Signal Processing Magazine*, *30*(2), 133-134. https://doi.org/10.1109/msp.2012.2230552

Stevenson, B. C., Borchers, D. L., Altwegg, R., Swift, R. J., Gillespie, D. M., & Measey, G. J. (2015). A general framework for animal density estimation from acoustic detections across a fixed microphone array. *Methods in Ecology and Evolution*, *6*(1), 38-48. https://doi.org/10.1111/2041-210X.12291

Su, Q., Shen, Y., Wei, Y., & Deng, C. (2017). Underdetermined blind source separation by a novel time-frequency method. *AEU - International Journal of Electronics and Communications*, *77*, 43-49. https://doi.org/10.1016/j.aeue.2017.04.025

Vincent, E., Gribonval, R., & Févotte, C. (2006). Performance measurement in blind audio source separation. *IEEE Transactions on Audio, Speech and Language Processing*, *14*(4), 1462-1469. https://doi.org/10.1109/TSA.2005.858005

Winter, S., Sawada, H., & Makino, S. (2006). Geometrical interpretation of the PCA subspace approach for overdetermined blind source separation. *Eurasip Journal on Applied Signal Processing*, *2006*, 1-11. https://doi.org/10.1155/ASP/2006/71632

Zhen, L., Peng, D., Yi, Z., Xiang, Y., & Chen, P. (2017). Underdetermined blind source separation using sparse coding. *IEEE Transactions on Neural Networks and Learning Systems*, *28*(12), 3102-3108. https://doi.org/10.1109/TNNLS.2016.2610960